CORONAL WAVES, SHOCK FORMATION AND CORONAL MASS EJECTIONS

Received: ……; Accepted: ……

Table of Contents

1	Shocks, blast waves, piston driven shocks	2
2	Identification of coronal waves	3
3	Lift-off and angular spread in the corona of flare/CME events. Are coronal waves tied with CME development?	3
4	Spectroscopic observations	5
5	SXT/radio observations of shock origins	5
6	Problems	6

Space Science Reviews **00:** 1–8, 2004.

1. Shocks, blast waves, piston driven shocks

Large-scale disturbances originating in flares or CMES propagate through a medium (the middle corona) that is not well understood quantitatively. As an MHD wave travels, it will in general steepen and form a shock; the existence of such shocks from global coronal waves was recognized early from the radio type II bursts, for which the high brightness temperatures and general morphology strongly suggested the presence of low-energy non-thermal electrons accelerated at a shock front. How the shock develops depends upon the nature of the medium in which the wave propagates. For a spherically-symmetric corona with no active regions, one would in general have an Alfvén speed v_A initially decreasing with height, then rising to a maximum in the near-Sun solar wind (Mann et al., 2003, as shown in Figure 1).

Gary (2001) provides more detail regarding the effects of an active region on the variation of plasma beta in the low corona; see Figure 2. Essentially an active region consists of a bubble of strong field embedded in the low corona; from the perspective of a coronagraph this bubble might be identified with a streamer base. A flare or CME typically originates in this low-beta, high v_A region and waves running away from it enter regions of lower Alfvén speed, leading to shock formation and to refraction as predicted by Uchida (1968). This refraction supports the identification of Moreton waves with global coronal waves, as Uchida proposed, and may have been identified directly in X-ray wave fronts by Hudson et al. (2003).

Type II radio emissions are caused by electrons accelerated by shocks at the local plasma frequency and/or its harmonic. They are usually observed below 400 MHz (Zlobec et al., 1993). Kilometric type II radio emissions from 30 KHz to a few MHz are produced in the interplanetary medium. Two types of shocks have been invoked to produce the type II bursts: the CME driving shocks associated with rising ejecta and the coronal shocks initiated during the impulsive phase of a flare. The association between type II bursts and shocks is rather complex, in particular in the corona where flares and CMEs often occur conjointly. Multiple type II bursts can be present in the same frequency range (see Figure 4 May 27 1999). Interaction of a shock wave with a coronal structure can trigger a secondary coronal shock as illustrated in Figure 5 for the February 18 2000 event. They can be detected in time and space coincidence with the propagation of a Moreton wave (see Figure 6, middle panel in Lift-off and angular spread in the corona of flare/CME events). Observations in the decametric-hectometric wavelength range showed that metric type II bursts, which are much more frequent than interplanetary type II bursts, do not generally extent up to hectometric wave lengths (Gopalswamy et al., 1998). There exists however a few observational evidences that coronal and interplanetary (IP) type II bursts can be produced during the same event and that multiple type II bursts can be present in the same frequency range. Radio imaging observations showed that some type II CME driven shocks can be produced at rather low alti-

tudes, below one solar radius in the corona. These bursts are weak and most often not detected by radio spectrographs.

2. Identification of coronal waves

Wave-like phenomena called EIT waves were discovered by the EUV Imaging Telescope (EIT) aboard the Solar and Heliospheric Observatory SOHO (Moses et al., 1997; Thompson et al., 1998). They typically appear as diffuse brightenings propagating nearly isotropically away from the site of active region transients, but avoiding strong magnetic features. Because of the rather poor temporal cadence of EIT, their speeds are difficult to determine and appear to be a few hundred km s ^{1}. The exact nature of these waves is not yet fully understood. It was suggested that they may be attributed to the compression of the plasma in the region surrounding the sudden magnetic field opening (Delannée, 2000). Dimmings seen in EUV were indeed found to be essentially restricted to the region traced by the propagation of these waves. A small number of EUV waves have sharp bright fronts, like the event presented in Figure 4 (Biesecker et al., 2002); it was proposed that these sharp EIT waves could be the coronal counterpart of H Moreton waves discovered by Moreton and Ramsey (1960) Moreton and Ramsey. Moreton waves are associated with large flares, have a More recently, observations of propagating disturbances in the corona, called X-ray waves, were detected in soft X-ray images from the *Yohkoh* Soft X-ray Telescope (SXT) (Khan and Aurass, 2002; Narukage et al., 2002, Hudson et al., 2003). These waves have sharp leading edges, are detected in coincidence with a Moreton wave and an EIT wave and are associated with radio metric type II bursts. An example is displayed in Figure 5.

We conclude that coronal (blast) waves which are the counterpart of the Moreton H waves have been unambiguously identified by their EUV and soft X ray emissions.

3. Lift-off and angular spread in the corona of flare/CME events. Are coronal waves tied with CME development?

The CME phenomenon results from the coupling of different spatial scales in the corona that go from the very small ones as current sheets, to active regions and filaments, up to very large transequatorial loops. Beside those CMEs which present a typical 3 part structure, other different types of CMEs have been identified. An initial mass ejection occurring to some latitude can lead to a further destabilisation of a much larger magnetic multipolar arch system and the resulting CME can reach angular extents exceeding 100 (e.g. Gosling 1997; Webb et al., 1997). Solar disk images in EUV, soft X-ray and radio have the possibility to image these different spatial scales and follow their evolution, if however the observing cadence is adequate. Many fast flares/CMEs are observed to start with a relatively small angular

size and reach their full extent in the low corona (below 2Rs) in a time scale of a few minutes. Nançay Radioheliograph (NRH) radio images showed that they initially originate from a rather small coronal region in the vicinity of the flare site and expand by successive magnetic interactions at progressively larger distances from the flare site. Signatures of these interactions are detected by bursts in the dm-m wavelength domain, (Maia et al., 1999). The time scale of this progression often corresponds to disturbances with speeds of 1000 km/s or more. Simultaneous on-the-disk H and radio observations of halo CMEs revealed that the radio sources are associated in space and time with the progression of a Moreton wave (see Figure 6). One important ouput of these studies was to establish that the angular extent of this class of CMEs is linked to the propagation of a coronal wave produced at the time of the flash phase of flares and producing further destabilization and magnetic interactions along its travelling path. These interactions lead to the production of secondary coronal shocks detected as radio type II bursts.The type II sources at one given frequency are not located radially above the flaring active centre but were resolved in multiple discrete components which spread along the wave front

Radio imaging observations provide an easy way to identify, visualise, ans follow the progression of coronal waves. Tracing the angular extents of associated CMEs is provided by one dimensional scans built from two dimensional images (Pick et al., 2003) and the corresponding speed of the disturbance can be easily estimated. The CME development in the corona takes place often within less than 10 minutes, much faster than the cadence of EIT and LASCO instruments. However, this result cannot be generalized. Triggering and angular extent of flare/CME events are not necessarily linked to the propagation of coronal waves. Another class of flare/CME events was recently identified (Maia et al., 2003). Figure 3 displays for the 14 October 1999 event, a composite image of an NRH image at 164 MHz and an LASCO C2 image; this event spanned over 90 in longitude; the two distant radio sources at the eastern (near the location of the flare) and western edges occurred quasi-simultaneously. Detailed analysis and modelling of the event revealed the presence of a coronal null point shown in Figure 3 . The observations are consistent with the occurrence of magnetic reconnection at this null point a few minutes before the beginning of the eruption. Both east and west activities would result in the propagation of MHD waves originating from the null point.

4. Spectroscopic observations

[place-holder words by HSH]

The UVCS instrument has actually detected coronal shocks spectroscopically, making identifications with type II bursts (Raymond et al., 2000; Mancuso et al., 2002). The results are consistent with a relatively weak shock, according to Uchida's picture. It is puzzling that more direct compressional signatures are not seen in the white-light images, but see Vourlidas et al. (2003).

5. SXT/radio observations of shock origins

Observations of wave propagation in the low corona (including the Moreton-wave signature in the chromosphere) offer us a chance to study the mechanism that launches the wave. The metric Type II burst often begins at a low frequency, implying a low density and a correspondingly high altitude. In part this must be because the "ignition" of the radio emission cannot start until the propagating disturbance actually reaches the shock condition (Vršnak, 2001).

Observations in the low corona and actually within the flaring volume thus offer the best possibility to identify the disturbance causing the wave(s) to propagate. Soft X-rays, microwaves, and EUV spectroscopy all provide tools that in principle can be used for this kind of study, but in practice the observations are extremely difficult because of the flare brightenings themselves. Furthermore there is a major complication from the nature of the medium we are observing. We believe that the plasma beta has low values within active regions, where flare disturbances typically occur. Thus the emitting features (loops and packets of plasma) do not themselves have a governing effect on the development of the motions. The magnetic field dominates, but it is not directly visible. We must thus consider all observed features in this domain to be tracers of the larger-scale development induced by the field restructuring. The restructuring of the field, i.e. motions locally perpendicular to the field, must ultimately launch the disturbance.

The *Yohkoh*/SXT soft X-ray telescope gave the first direct coronal X-ray observations with high time resolution, and it seemed reasonable that should cleanly show Uchida's fast-mode shocks if they were at a high enough Mach number. This expectation was defeated by several factors, including the telescope's scattering halo produced from the flare itself (Hudson et al., 2003). On the plus side, the SXT observations allowed for searches well inside the distance needed for type II ignition. Several waves have been detected (Khan and Aurass, 2002, Narukage et al., 2002, Hudson et al., 2003), and have the expected relationships with Moreton waves and type II bursts. The observation of the 1998 May 6 event (Hudson et al., 2003) showed the expected refractive tilting of the wave front as expected from the active-region magnetic structure (e.g., (Gary, 2001)). We illustrate this in Figure 10.

The significance of such observations, and perhaps microwave observations (S. White, personal communication 2004) is that they reveal the presence of the disturbance(s) close to the core brightening of the flare. The X-ray observations also show the early development of ejection signatures closely related to CME eruption (e.g., Nitta and Akiyama, 1999), and so they allow a close-in distinction between a free-running blast wave and a standoff wave resulting from the mass ejection. This distinction was clear for the 1998 May 6 event (Hudson et al., 2003), because the two disturbances propagated almost orthogonally to one another.

6. Problems

* Have Vourlidas et al. (2003) really detected a coronal wave in white light? Why does it look so odd and why is their observation so singular?
* How are the observations in the low corona, which show weak shocks, to be reconciled with diffusive shock acceleration theory, which requires strong shocks?
* Why do even feeble flares occasionally have blast-wave signatures?
* What is the physics of the type II precursor (e.g., Klassen et al., 2003)?
* What is the nature of the motions that launch the blast wave?

References

Delannée, C.: 2000, 'Another View of the EIT Wave Phenomenon'. *ApJ* **545**, 512–523.

Gary, G. A.: 2001, 'Plasma Beta above a Solar Active Region: Rethinking the Paradigm'. *Solar Phys* **203**, 71–86.

Gopalswamy, N., M. L. Kaiser, R. P. Lepping, S. W. Kahler, K. Ogilvie, D. Berdichevsky, T. Kondo, T. Isobe, and M. Akioka: 1998, 'Origin of coronal and interplanetary shocks - A new look with WIND spacecraft data'. *JGR* **103**, 307–+.

Hudson, H. S., J. I. Khan, J. R. Lemen, N. V. Nitta, and Y. Uchida: 2003, 'Soft X-ray observation of a large-scale coronal wave and its exciter'. *Solar Phys* **212**, 121–149.

Khan, J. I. and H. Aurass: 2002, 'X-ray observations of a large-scale solar coronal shock wave'. *A&A* **383**.

Klassen, A., S. Pohjolainen, and K.-L. Klein: 2003, 'Type II radio precursor and X-ray flare emission'. *Solar Phys* **218**, 197–210.

Maia, D., A. Vourlidas, M. Pick, R. Howard, R. Schwenn, and A. Magalhães: 1999, 'Radio signatures of a fast coronal mass ejection development on November 6, 1997'. *JGR* **104**, 12507–12514.

Mancuso, S., J. C. Raymond, J. Kohl, Y.-K. Ko, M. Uzzo, and R. Wu: 2002, 'UVCS/SOHO observations of a CME-driven shock: Consequences on ion heating mechanisms behind a coronal shock'. *A&A* **383**, 267–274.

Mann, G., A. Klassen, H. Aurass, and H.-T. Classen: 2003, 'Formation and development of shock waves in the solar corona and the near-Sun interplanetary space'. *A&A* **400**, 329–336.

Moreton, G. E. and H. E. Ramsey: 1960, 'Recent Observations of Dynamical Phenomena Associated with Solar Flares'. *PASP* **72**, 357–+.

Narukage, N., H. S. Hudson, T. Morimoto, S. Akiyama, R. Kitai, H. Kurokawa, and K. Shibata: 2002, 'Simultaneous Observation of a Moreton Wave on 1997 November 3 in H and Soft X-Rays'. *ApJL* **572**, L109–L112.

Nitta, N. and S. Akiyama: 1999, 'Relation between Flare-associated X-Ray Ejections and Coronal Mass Ejections'. *ApJL* **525**, L57–L60.

Raymond, J. C., B. J. Thompson, O. C. St. Cyr, N. Gopalswamy, S. Kahler, M. Kaiser, A. Lara, A. Ciaravella, M. Romoli, and R. O'Neal: 2000, 'SOHO and radio observations of a CME shock wave'. *GRL* **27**, 1439–1442.

Uchida, Y.: 1968, 'Propagation of Hydromagnetic Disturbances in the Solar Corona and Moreton's Wave Phenomenon'. *Solar Phys* **4**, 30–+.

Vourlidas, A., S. T. Wu, A. H. Wang, P. Subramanian, and R. A. Howard: 2003, 'Direct Detection of a Coronal Mass Ejection-Associated Shock in Large Angle and Spectrometric Coronagraph Experiment White-Light Images'. *ApJ* **598**, 1392–1402.

Vršnak, B.: 2001, 'Solar flares and coronal shock waves'. *JGR* **106**, 25291–25300.

Zlobec, P., M. Messerotti, M. Karlicky, and H. Urbarz: 1993, 'Fine structures in time profiles of type II bursts at frequencies above 200 MHz'. *Solar Phys* **144**, 373–384.

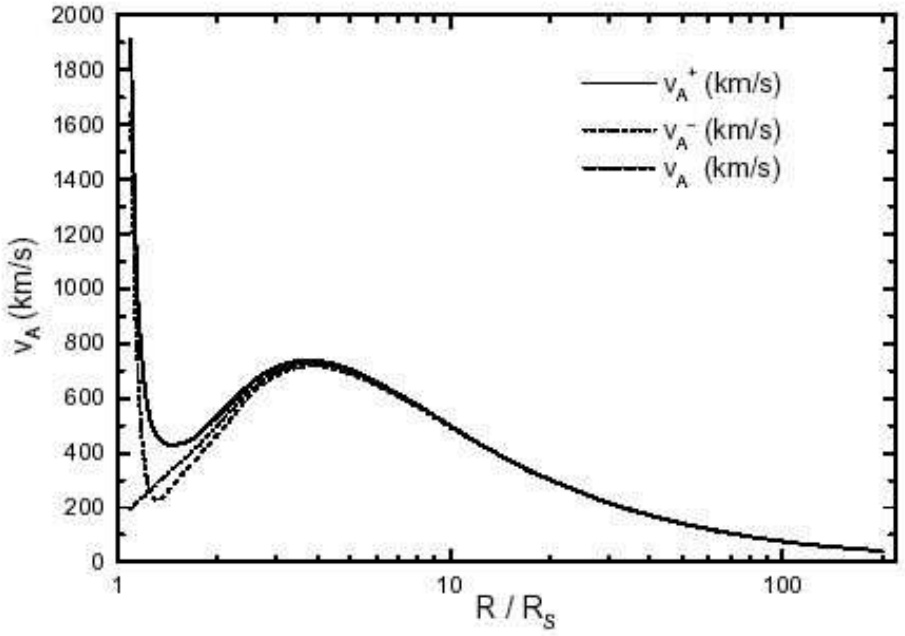

Figure 1. Variation of coronal Alfvèn speed with height, as estimated by Mann et al. (2003). The C and refer to the orientation of the assumed active-region dipole of the model relative to the coronal field. The dotted line approaching low values at 1.0 R_0 is for the quiet corona alone.

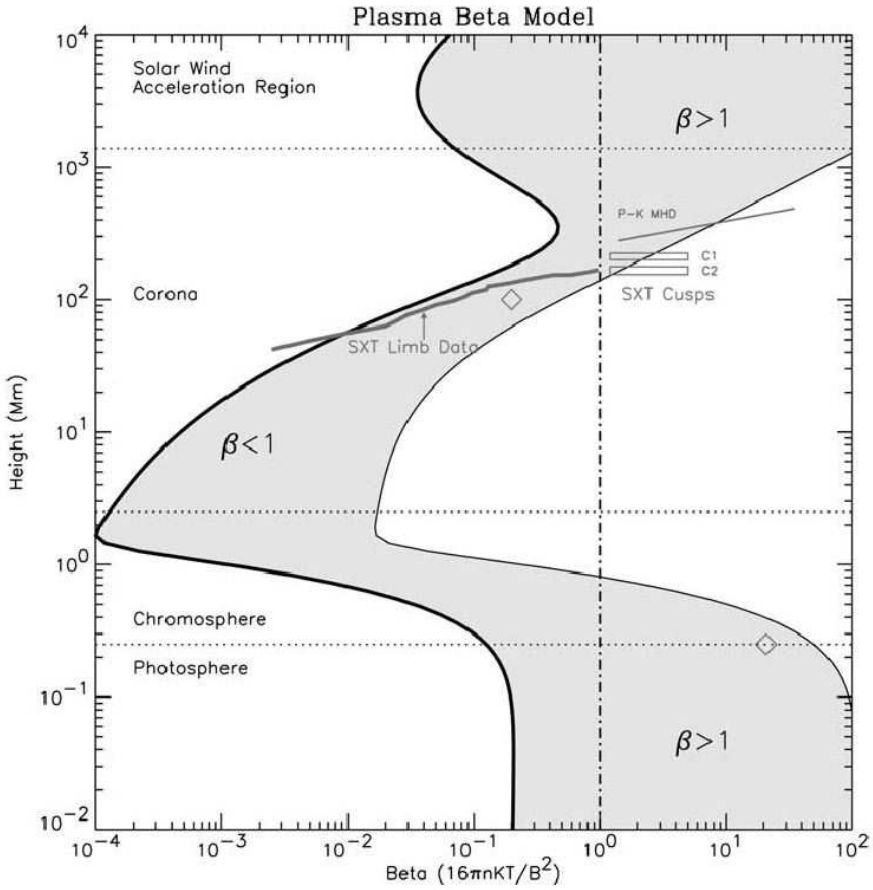

Figure 2. Variation of coronal plasma beta in the corona around an active region, as estimated by Gary (2001), and which he used to interpret the X-ray cusp structures often seen in physically large flares with *Yohkoh* SXT data.

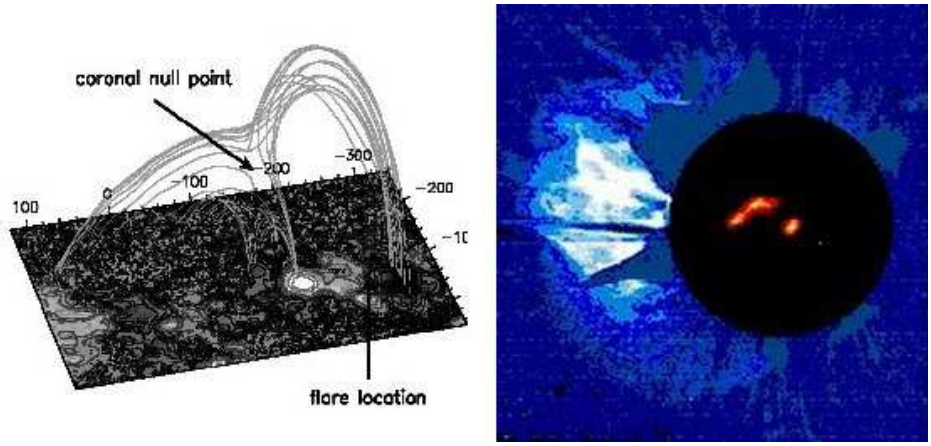

Figure 3. 14 October 1999 event. *left* : SOHO/MDI magnetogram (Scherrer et al., 1995) overlaid by some calculated field lines showing the existence of a magnetic null point located between the two east and west edges of the active region; the magnetogram shows the extent of the active region. *right* : composite image of one C2 image with one radio image at 164 MHz. This event spanned 90 degrees in longitude. The two radio sources at the eastern and western edges illuminated quasi-simultaneously (from Maia et al., 2003).

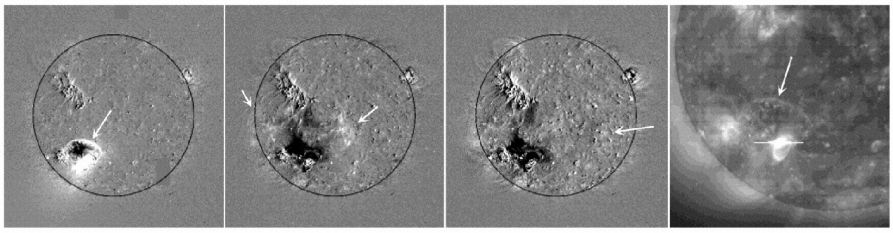

Figure 4. Example of an EIT wave from September 24 1997. The first three panels show successive EIT images at 02:49, 03:03, and 03:23 UT with a pre-event image digitally differenced from them. Arrows indicate the EIT-wave front(s). The last panel shows a subfield of the first panel (undifferenced), showing an example of a sharp brightening (from Biesecker et al., 2001).

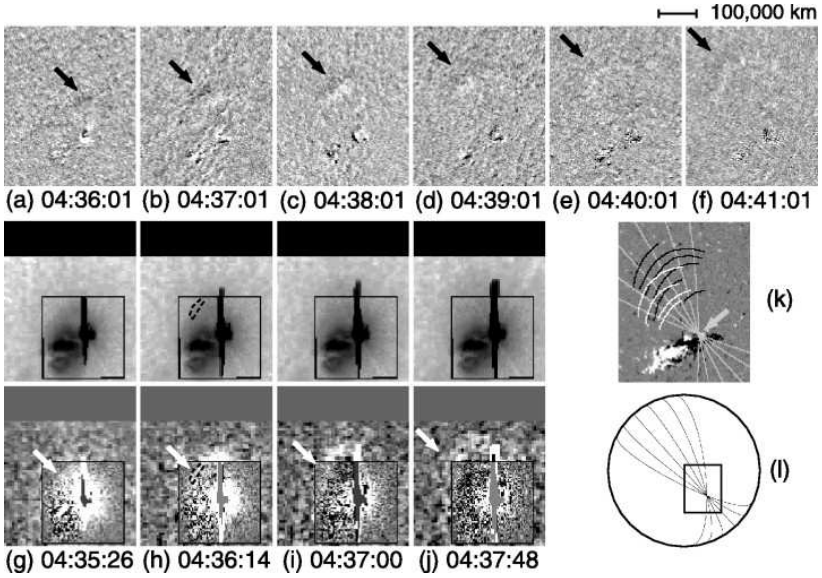

Figure 5. Observed images on November 3 1997 at NOAA AR 8100 (a-f) H + 0.8Årunning difference images of a Moreton wave (*black arrows*). (g-f) Soft X-ray (*middle panels*) and running difference (*bottom panels*) image of an X-ray wave (*white arrows*) taken with the AlMg filter. The images inside and outside the boxes are half resolution ($4.91''$) and quarter-resolution ($9.82''$) images, respectively. (k) Wave fronts of the Moreton wave at every minute from 04:36:01 to 04:41:01 UT (*black lines*) and the X-ray wave at 04:35:26, 04:36:14, 04:37:00, and 04:37:48: UT (*white lines*) overlaid on the photospheric magnetic field observed at 04:51:04. Gray lines show the great circles through the flare site (*gray arrow*). The rectangle, circle, and lines shown in (l) are the field of view of (a)-(k), the limb of the Sun, and the great circles, respectively (from Narukage et al., 2002).

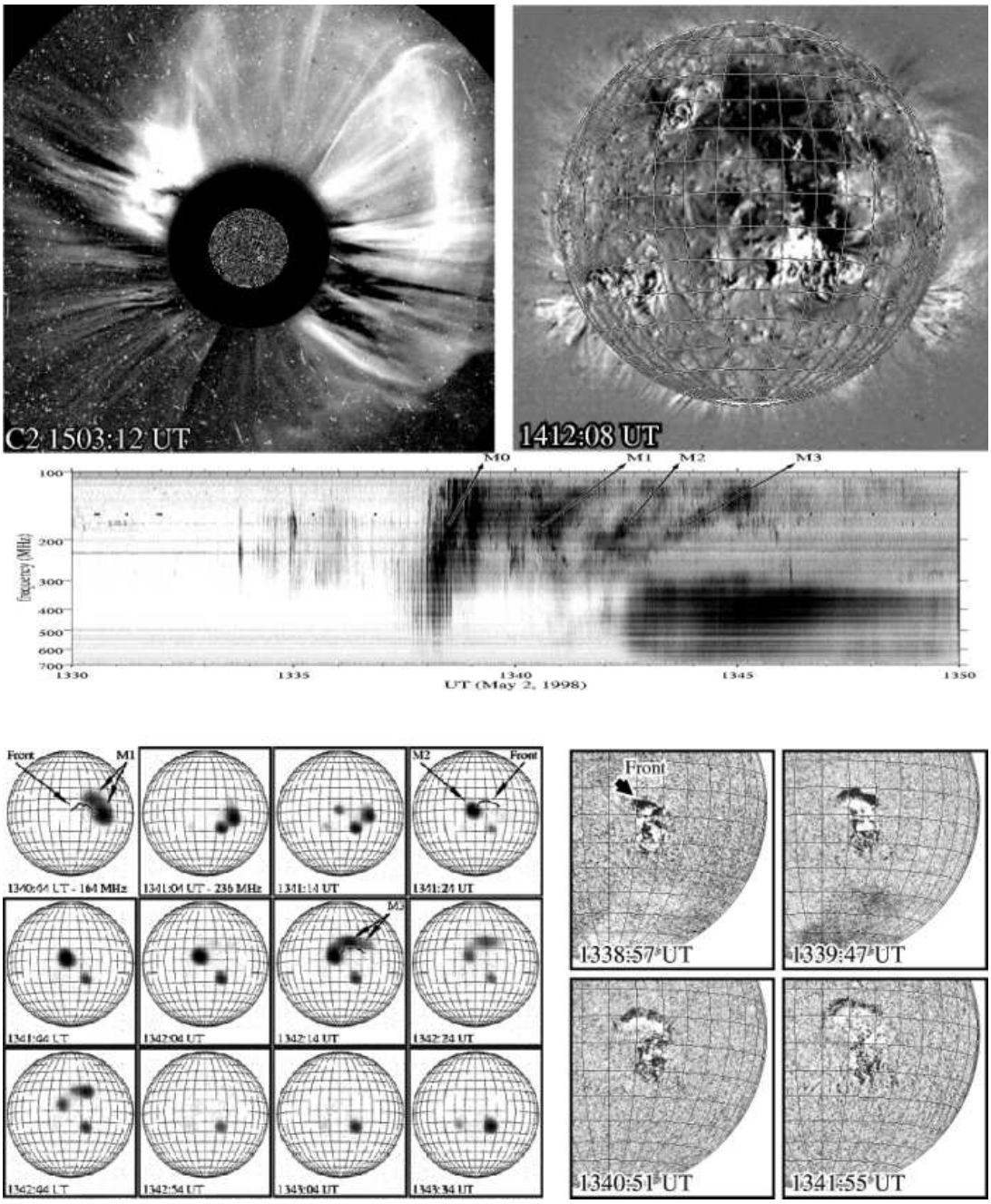

Figure 6. Upper panel, left: SOHO LASCO C2 image showing the halo CME on May 2). *Upper panel right*: SOHO EIT at 195Åshowing the EIT dimming region. *Middle panel*: Artemis IV radio spectra : the spectral drifting sources are labelled M0 for the one in the flash phase and M1, M2, M3 for the type II-like emission. *Lower panel, right*: Running difference of Kanzelhohe H images showing the moving wave front (marked by an arrow in the first difference image). Nançay Radio heliograph images at 164 MHz and 236 MHz showing the location of the sources labelled M1, M2, M3 at selected times (adapted from Pohjolainen et al., 2001).

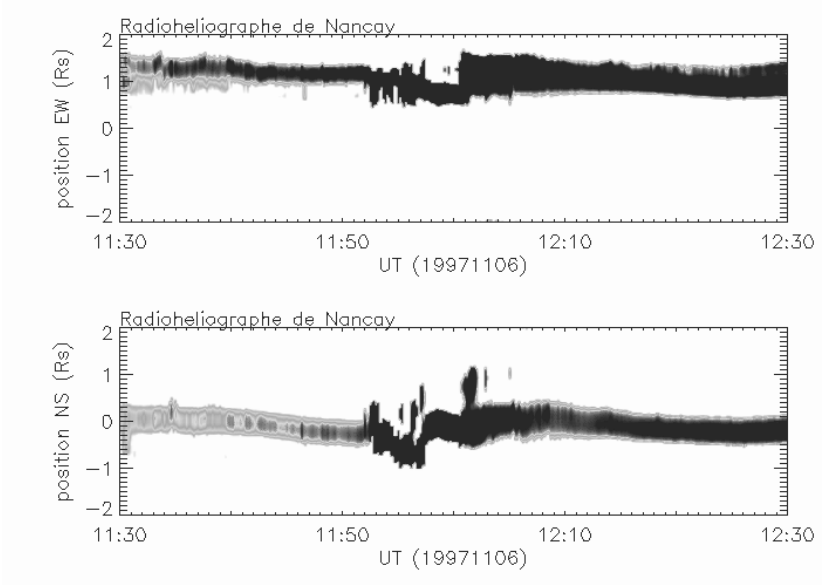

Figure 7. November 06 1997. Multiple loop systems participate to this development. Two one-dimensional images plots along east-west(top) and north-south (bottom) directions showing the space-time evolution of the event at 164 MHz.Sources of bursts are organized in a series of discrete distinct features. Their drift in position provides an estimate of the projected speed of the associated coronal wave (from Pick et al., 2003).

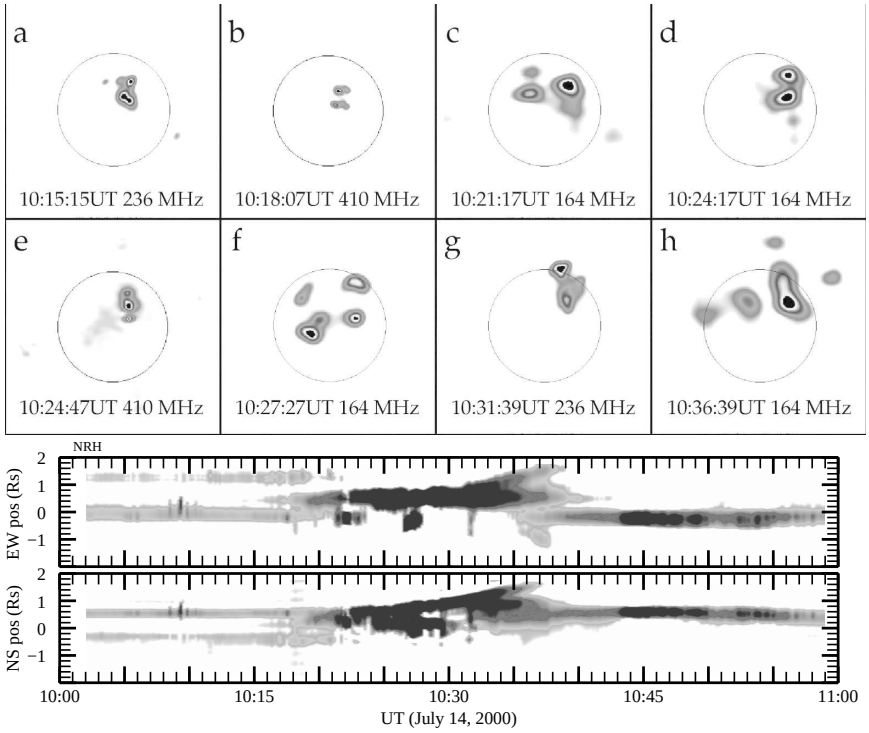

Figure 8. 14 July 2002. Top: radio images at 164 MHz showing the on-disk progression of the event. Bottom: space-time evolution of the event along the east-west and south-north directions showing its on-the-disk progression.

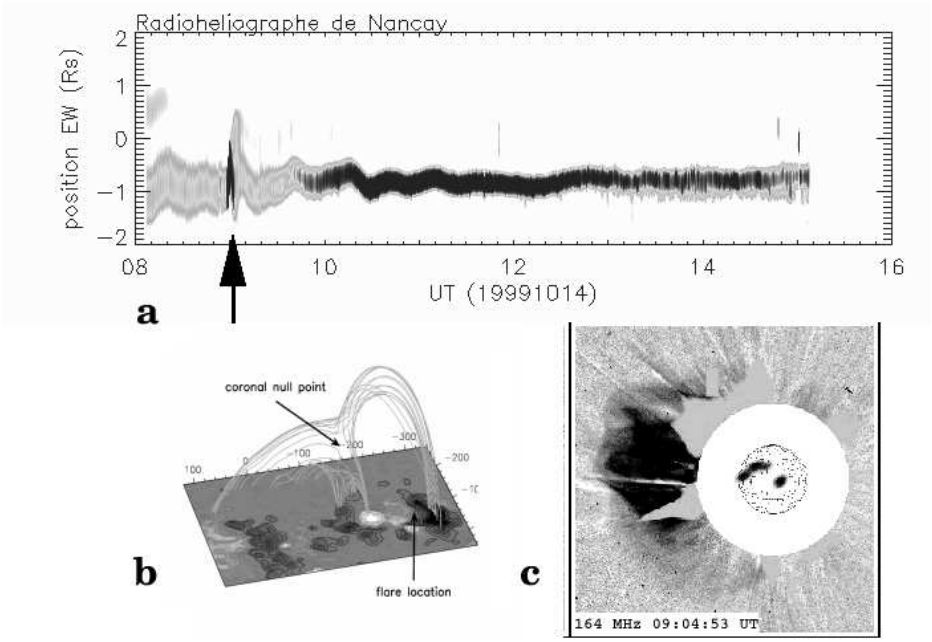

Figure 9. 14 October 1999 event. *Fig. 3a* : radio signature of the east-west extent of the event, see the arrow. *Fig. 3b* : SOHO/MDI magnetogram (Scherrer et al., 1995) overlaid by some calculated field lines showing the existence of a magnetic null point located between the two east and west edges of the active region; the magnetogram shows the extent of the active region. *Fig. 3c* : composite image of one C2 image with one radio image at 164 MHz (from Maia et al., 2002).

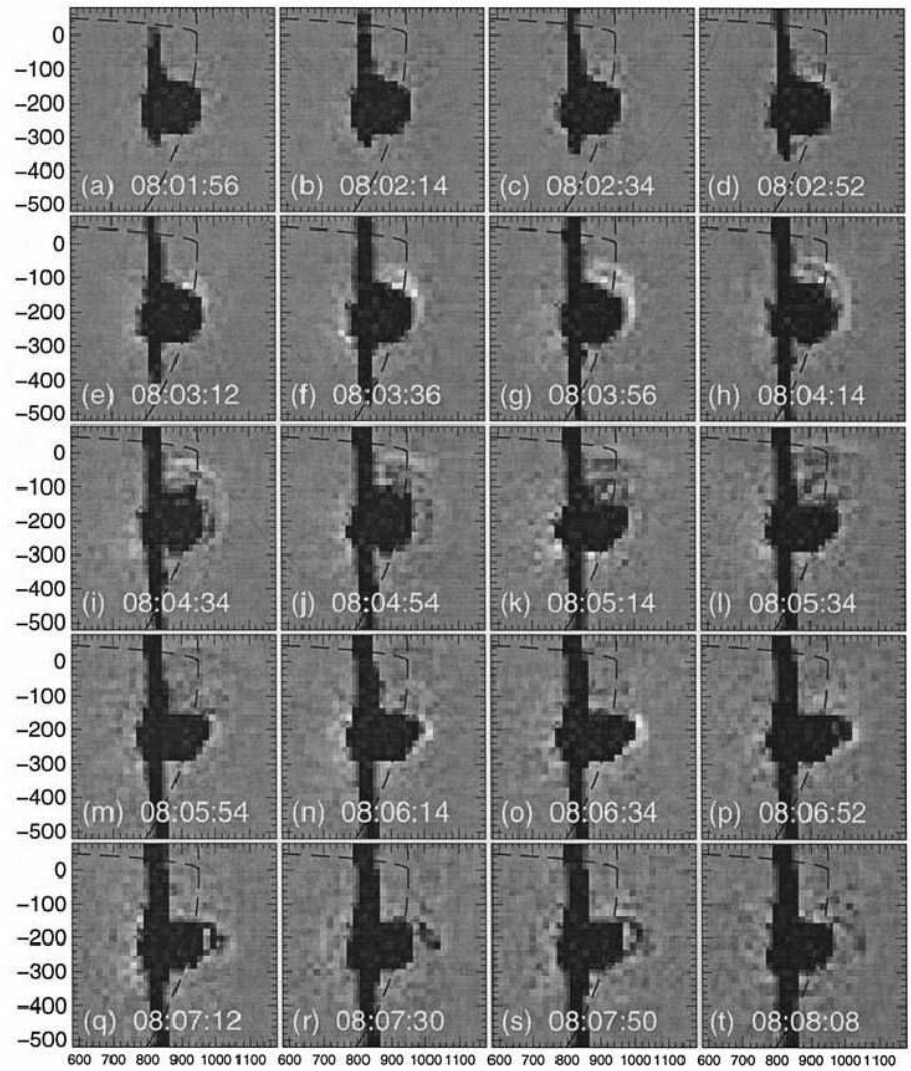

Figure 10. X-ray observations of a coronal wave originating in an X-class flare on 1998 May 6 (Hudson et al., 2003). The dashed line shows the solar west limb and one parallel. These are running difference images. They show the expected wave-front tilting (see the panel at 08:05:14 UT, for example. The flare ejecta occur later and in a different direction (frame at 08:07:12 UT, for example).